CrossMark

ORIGINAL ARTICLE

Indirubin Inhibits LPS-Induced Inflammation *via* TLR4 Abrogation Mediated by the NF-kB and MAPK Signaling Pathways

Jin-lun Lai,[1] Yu-hui Liu,[1] Chang Liu,[1] Ming-pu Qi,[1] Rui-ning Liu,[1] Xi-fang Zhu,[1] Qiu-ge Zhou,[1] Ying-yu Chen,[1,2] Ai-zhen Guo,[1,2,3] and Chang-min Hu[1,2,3]

Abstract—Indirubin plays an important role in the treatment of many chronic diseases and exhibits strong anti-inflammatory activity. However, the molecular mode of action during mastitis prophylaxis remains poorly understood. In this study, a lipopolysaccharide (LPS)-induced mastitis mouse model showed that indirubin attenuated histopathological changes in the mammary gland, local tissue necrosis, and neutrophil infiltration. Moreover, indirubin significantly downregulated the production of interleukin (IL)-1β, IL-6, and tumor necrosis factor-α (TNF-α). We explored the mechanism whereby indirubin exerts protective effects against LPS-induced inflammation of mouse mammary epithelial cells (MMECs). The addition of different concentrations of indirubin before exposure of cells to LPS for 1 h significantly attenuated inflammation and reduced the concentrations of the three inflammatory cytokines in a dose-dependent manner. Indirubin downregulated LPS-induced cyclooxygenase-2 (COX-2) and Toll-like receptor 4 (TLR4) expression, inhibited phosphorylation of the LPS-induced nuclear transcription factor-kappa B (NF-kB) P65 protein and its inhibitor IkBα of the NF-kB signaling pathway. Furthermore, indirubin suppressed phosphorylation of P38, extracellular signal-regulated kinase (ERK), and c-Jun NH$_2$-terminal kinase (JNK) of the mitogen-activated protein kinase (MAPK) signal pathways. Thus, indirubin effectively suppressed LPS-induced inflammation *via* TLR4 abrogation mediated by the NF-kB and MAPK signaling pathways and may be useful for mastitis prophylaxis.

KEY WORDS: indirubin; lipopolysaccharide (LPS); TLR4; NF-kB; MAPK; inflammation.

INTRODUCTION

Mastitis is one of the most costly diseases of dairy cattle [1]. Inflammation of the mammary gland has nega-

[1] The Faculty of Veterinary Medicine, Huazhong Agricultural University, Wuhan, 430070, China

[2] State Key Laboratory of Agricultural Microbiology, Huazhong Agricultural University, Wuhan, 430070, China

[3] To whom correspondence should be addressed at The Faculty of Veterinary Medicine, Huazhong Agricultural University, Wuhan, 430070, China. E-mails: aizhen@mail.hzau.edu.cn; hcm@mail.hzau.edu.cn

tive physical, chemical, and biological consequences [2]. Many microorganisms, including the Gram-positive *Staphylococcus aureus* and the Gram-negative *Escherichia coli*, can cause mastitis [3–6]. *E. coli* is a major cause of bovine mastitis, particularly around the time of parturition or during early lactation [7]. Lipopolysaccharide (LPS), a principal component of the outer membrane of Gram-negative bacteria, triggers mastitis in bovine and mouse models and induces the production of various pro-inflammatory cytokines. LPS is a key trigger of inflammation [8]. The innate immune system plays an important role in defense against invading pathogens. Mouse mammary epithelial cell (MMEC) cultures are widely used to study the capacity of cells to sense and respond to mastitis-causing bacteria [9]. Such MMECs are the first line of defense against

mammary bacterial infection, recognizing molecules typical of microbes *via* Toll-like receptors (TLRs) and other pattern recognition receptors (PRRs) [10]. TLR4, a key PRR, binds and contacts downstream mitogen-activated protein kinases (MAPKs) and nuclear transcription factor-kappa B (NF-kB) *via* receptor dimerization [11]. Activated MAPKs and components of the NF-kB signaling pathway regulate inflammation by promoting the expression of interleukin (IL)-1β, IL-6, tumor necrosis factor-α (TNF-α), and other pro-inflammatory cytokines [12, 13]. Because a serious inflammatory reaction can cause major tissue damage, medicines that inhibit the activation of the TLR4 signaling pathway are potential anti-inflammatory agents and may prevent tissue damage caused by mastitis [14].

Indirubin, a 3,20 *bis*-indole isomer of indigo, is an active ingredient of Danggui Longhui Wan, a traditional Chinese medicine derived from a mixture of plants including *Indigofera tinctoria* L., *Isatis tinctoria* L., *Strobilanthes cusia* Kuntze, and *Cnidii fructus* [15]. Indirubin exhibits anti-leukemic, anti-proliferative, and hepatoprotective properties and is also a strong anti-inflammatory agent [16–22]. In this study, we investigated the protective properties of indirubin against mastitis caused by a LPS-induced inflammatory response, and we elucidated the associated anti-inflammatory mechanisms.

MATERIALS AND METHODS

Chemical and Reagents

Indirubin (HPLC ≥ 98 %) was purchased from Shanghai Yuanye Biological Technology Co., Ltd. (Shanghai, China) (Fig. 1). Fetal bovine serum (FBS) and 0.25 % trypsin-EDTA were purchased from Gibco (Grand Island, NY, USA). LPS (*E. coli* 055:B5), human epidermal growth factor (EGF), insulin, and transferrin were purchased from Sigma Chemical Co. (St. Louis, MO, USA). Dulbecco's modified Eagle's medium (DMEM/F12/1:1) was purchased from Thermo Fisher Biochemical Products Co., Ltd. (Beijing, China). 3-(4,5-Dimethyl-2-thiazolyl)-2,5-diphenyl-2-*H*-tetrazolium bromide (MTT) cell counting kit, HiScript® II RT SuperMix for PCR (R212-01) and AceQ qPCR SYBR Green Master Mix (Q111-02) were purchased from Vazyme Biotech Co., Ltd. (Nanjing, China). Mouse IL-1β platinum ELISA kit with pre-coated plates was purchased from eBioscience (San Diego, CA, USA). Mouse IL-6 and TNF-α platinum ELISA kits with pre-coated plates come from BioLegend (San Diego, CA,
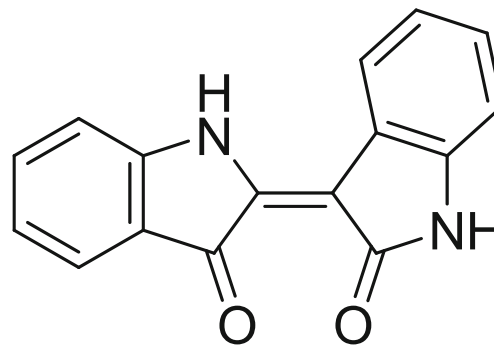

Fig. 1. Chemical structure of indirubin.

USA). β-Actin (BA2305) was purchased from Wuhan Boster Biological Engineering Co., Ltd. (Wuhan, Hubei, China); PTGS2 (cyclooxygenase-2 (COX-2)) and anti-TLR4 antibodies were purchased from GeneTex, Inc. (San Antonio, TX, USA). NF-kB pathway sampler kit was purchased from Cell Signaling Technology, Inc. (Beverly, MA, USA). MAPK family antibody sampler kit and phospho-MAPK family antibody sampler kit were purchased from Arigo (Taiwan, China).

In Vivo Study

Experimental Design

All animal procedures were approved by the Animal Welfare and Research Ethics Committee of Huazhong Agricultural University. Mastitis was induced in the L4 and R4 abdominal mammary glands of the mice models through an inoculate of 50 μL of 0.2 mg/mL LPS, as described previously [23]. Briefly, mice were separated from their offspring approximately 2 h prior to anesthetization with pentobarbital sodium salt (0.25 g pentobarbital sodium salt dissolved in 50 mL phosphate-buffered saline (PBS), 10 mg per 20 g i.p.). Thirty-six Kunming pregnant mice were purchased from the Center for Animal Experiment and ABSL-3 Laboratory of WHU (Hubei, China) and randomly divided into six groups: control group, dimethyl sulfoxide (DMSO) group, LPS group, 25 μM indirubin and LPS group, 50 μM indirubin and LPS group, and 100 μM indirubin and LPS group. LPS groups were used as positive controls. Different concentrations of indirubin and 0.1 % DMSO were administered by intraperitoneal injection approximately 1 h before and 12 h after LPS instillation, respectively. The control and LPS groups were given equivalent volumes of PBS. Following the LPS challenge after 24 h, the mice were euthanized by CO_2, and then mammary gland tissue was

harvested and stored at −80 °C in a cell-frozen storage tube freezer.

Detection of Inflammatory Cytokine Levels

Each mammary gland tissue sample was weighed and homogenized with phosphate buffer (*w/v*, 1:9) on crushed ice and then ground using a tissue homogenizer. Tissue samples were centrifuged at 2000*g* for 40 min at 4 °C, the lipid was discarded, and the supernatant was collected and centrifuged again at 2000*g* for 20 min at 4 °C to remove any remaining lipid. The supernatant was used to detect IL-1β, IL-6, and TNF-α levels in the mammary gland tissue using ELISA following the kit manufacturer's instructions.

Histopathologic Evaluation of Mammary Gland Tissue

Mammary gland tissues were harvested 24 h after the LPS challenge for histopathological examination. The tissue samples were fixed in 4 % paraformaldehyde for 48–72 h, dehydrated with graded alcohol, embedded in paraffin, and then stained with hematoxylin (H) and eosin (E).

In Vitro Study

Experimental Design

Indirubin was dissolved in DMSO at 5–15 mM, stored in aliquots at −20 °C, and further diluted (as appropriate) in a culture medium. Primary MMECs were isolated, cultured to 80–85 % confluence, and divided into the following groups:

(1) Indirubin + LPS group (indirubin + LPS): MMECs were pretreated with indirubin at 25, 50, or 100 nM for 1 h and stimulated with LPS (1 μg/mL) for 24 h.
(2) Indirubin group (indirubin): MMECs were cultured with 25, 50, or 100 nM indirubin for 24 h.
(3) DMSO group (DMSO): MMECs were cultured with 0.1 % (*v/v*) DMSO for 24 h.
(4) Control group (Con): MMECs were treated with a cell culture medium (vehicle control) of the same volume, for the same time, as the other groups.
(5) LPS group (LPS): MMECs were stimulated with LPS (1 μg/mL) for 24 h as a positive group.

Primary MMEC Isolation and Culture

MMECs were isolated following a previously described method [24] with slight changes. In brief, the fourth and fifth mouse mammary tissues were aseptically harvested from the mice after 18 to 20 days of pregnancy. Tissue fragments were washed in PBS with 2 % (*w/v*) penicillin-streptomycin until the wash solutions were clear and then minced using surgical scissors, and the minced samples were digested for 3 h at 37 °C at 110 revolutions/min in an oscillating incubator. The digestion mix was 0.2 % (*w/v*) each of collagenases I and II in 45 mL DMEM/F12 and 5 mL FBS (sterilized by filtering through a 0.45-μm-pore-sized filter) and 0.25 % (*w/v*) trypsin-EDTA. Each digest was centrifuged at 250*g* for 5 min and filtered through a 70-μm-pore-sized nylon mesh (Falcon). Each filtrate was digested with 0.25 % (*w/v*) trypsin-EDTA and filtered through a 40-μm-pore-sized nylon Tamis cell strainer to remove epithelial organoids. Differential adhesion was used to remove fibroblasts, red blood cells, and endothelial cells (which attached to the tube walls at different times). Primary MMECs were cultured in the basic serum-free medium DMEM/F12 (1:1) containing 5 ng/mL EGF, 5 μg/mL insulin, 5 μg/mL transferrin, 10 % (*v/v*) fetal bovine serum, and 1 % (*w/v*) penicillin-streptomycin, at 37 °C under 5 % (*v/v*) CO_2 in a humidified atmosphere.

MTT Assay of Cell Viability

The effect of indirubin on primary MMEC viability was measured using the standard MTT assay as previously described [14]. In brief, 1×10^4 MMECs were seeded into 96-well plates for 24 h, indirubin and LPS were added or were not added, and incubation was continued for an additional time of 24 h. Indirubin was dissolved in DMSO; however, the DMSO concentration in the assay was <0.1 %; 0.1 % (*v/v*) DMSO thus served as the control. MTT was added (to 5 % *w/v*) to each well, and the culture was continued for 4 h. The medium was removed, and the cells were washed three times with PBS. The formazan crystals were dissolved in 150 μL DMSO/well; the absorbance was acquired at 570 nm using a microplate reader.

Total RNA Extraction and qRT-PCR

Total RNA extraction and qRT-PCR followed as previously described [25] with slight changes. In short, MMECs (1×10^6) were seeded into six-well plates and grown until 80–85 % confluent. Indirubin and LPS were added or were not added, and incubation was continued for an additional time of 24 h. The cells were washed twice with ice-cold PBS; 1 mL of the TRIzol (Molecular Research Center, USA) reagent was added to each well and processed as directed by the manufacturer, and the cell lysates were collected. Genomic DNA was removed from all samples by treatment with 4× genomic DNA (gDNA) wiper mix, and RNA was reverse-transcribed into

complementary DNA (cDNA) using the HiScript® II QRT SuperMix for qPCR (with the gDNA wiper). Relative mRNA concentrations were quantitated and subjected to qRT-PCR using the ViiA™ 7 system (Applied Biosystems), SYBR® Green Master Mix, and the platinum SYBR Green qPCR Super Mix with 6-carboxyl-X-rhodamine II (ROX II), following the manufacturer's instructions (Vazyme Biotech Co., Ltd., Nanjing, China). The primers used are listed in Table 1 [26–29]. The PCR cycling conditions were 2 min at 50 °C followed by 2 min at 95 °C and then 40 cycles of 15 s at 95 °C, 30 s at 58 °C, and 30 s at 72 °C. Each reaction mixture contained 1 μL of cDNA, 5 μL of the SYBR Green Super Mix, and sense and anti-sense primers. Each sample was run three times in triplicate; the data were averaged. Melting curves were constructed to assess PCR accuracy. The $2^{-\Delta\Delta Ct}$ method was used to measure the expression levels of calibrator genes. β-Actin served as an internal control. We calculated ΔCt values as follows: $\Delta Ct = Ct$ (target gene) $- Ct$ (housekeeping gene) and also the following: $\Delta\Delta Ct = \Delta Ct$ (treatment) $- \Delta Ct$ (control). Amplitude variation served as a surrogate measure of gene expression.

Enzyme-Linked Immunosorbent Assay

MMECs (1×10^6) were seeded into six-well plates and grown until 80–85 % confluent; indirubin and 1 μg/mL LPS were added or were not added, and incubation was continued for an additional time of 24 h. Cell-free supernatants were subsequently used for the pro-inflammatory cytokine assays with mouse ELISA kits according to the manufacturer's instructions.

Western Blotting

MMECs (1×10^6) were seeded into six-well plates and grown until 80–85 % confluent; indirubin and 1 μg/mL LPS were added or were not added, and incubation was continued for an additional time of 24 h. The cells were washed twice with ice-cold PBS. Total proteins were extracted via rapid lysis. Protein extraction reagent was added to lysates on ice, followed by centrifugation at 12,000g for 10 min to collect supernatants. The proteins were quantitated using the BCA protein assay. Equal amounts of protein (20–30 μg) were loaded onto a 10 % (w/v) SDS-polyacrylamide gel, electrophoresed, and transferred to polyvinylidene difluoride membranes. The membranes were blocked with 5 % (w/v) BSA (Bio-Sharp) with Tris-buffered saline (TBST) containing 0.05 % (v/v) Tween-20 at room temperature for 3 h and then washed three times with TBST for 10 min each time. Primary antibodies were diluted in TBST and incubated with the membrane overnight, shaking at 4 °C. Each membrane was then washed with TBST followed by incubation with an HRP-conjugated secondary antibody at room temperature for 1 h while shaking. Finally, each membrane was developed using an enhanced chemiluminescence (ECL) detection kit and visualized using a chemiluminescence detection system (ChemiDoc; Bio-Rad, USA). Band densities were calculated using ImageJ software (BioTechniques, NY, USA).
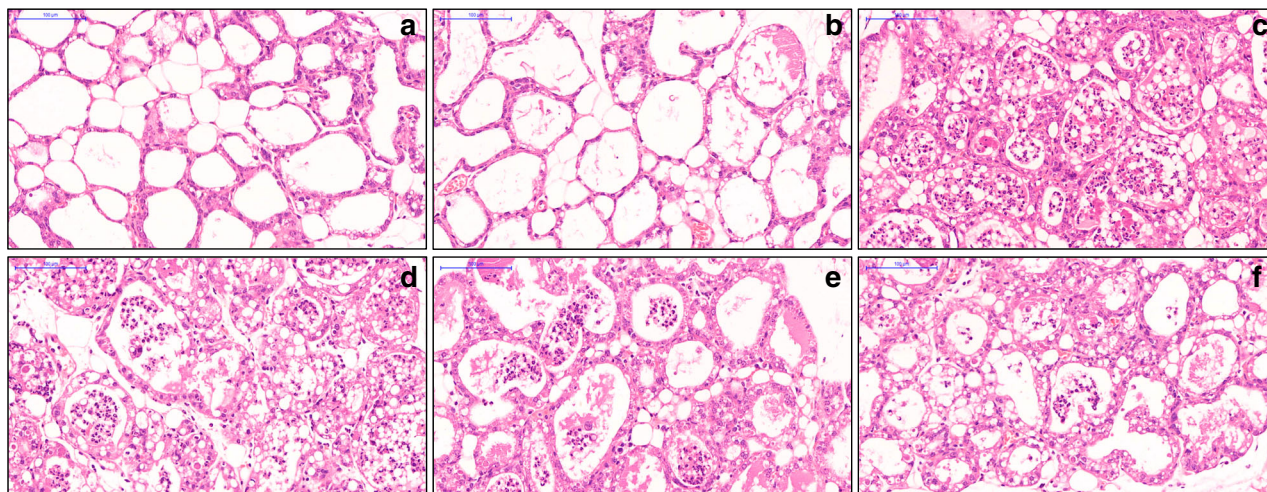
Statistical Analysis

All data are expressed as the means ± SEMs and were compared by one-way analysis of variance (ANOVA, Dunnett's t test). A p value <0.05 was considered to reflect statistical significance.

RESULTS

Histological Analysis of Mammary Gland Tissue

Histological analysis is the most direct method for evaluating tissue injury and indirubin treatment effects. Pathological changes and inflammatory cells were negligible in the control (Fig. 2a) and DMSO (Fig. 2b) groups. However, in the LPS groups, the mammary alveolus was hyperemic and thicker than the alveolus space and neutrophil infiltration (Fig. 2c). The indirubin ameliorated LPS-induced pathological changes in a dose-dependent manner (Fig. 2d–f). Furthermore, we observed fewer neutrophils and macrophages in the alveolus space as well as reduced

Table 1. Sequence of Primers Used in the Current Investigation in qRT-PCR

Gene	Primers sequence (5'→3)	
β-Actin	F:TGCTGTCCCT GTATGCCTCT	R:GGTCTTTACGGA TGTCAACG
TNF-α	F:CGATGAGGT CAATCTGCCCA	R:CCAGGTCACTGT CCCAGC
IL-1β	F:TGAAATGCCACCT TTTGACAG	R:CCACAGCCACAA TGAGTGATAC
IL-6	F:TGCCTTCTTGGGACTGAT	R:CTGGCTTTGTCT TTCTTGTT
COX-2	F:CCAGCACTTCA CCCATCAGTT	R:ACCCAGGTCCTC GCTTATGA

F forward, *R* reverse

Fig. 2. Effect of indirubin on histological changes in LPS-induced mastitis mice. Different concentrations of indirubin (25, 50, and 100 μM) were given by i.p. injection 1 h before and 12 h after LPS administration. Mouse mammary glands (*n* = 3–5) from each experimental group were processed for histological evaluation at 24 h after LPS challenge. Representative histological changes of the mammary gland from different groups: **a** control group, **b** DMSO group, **c** LPS group, **d** indirubin (25 μM) and LPS group, **e** indirubin (50 μM) and LPS group, and **f** indirubin (100 μM) and LPS group, all intervals of 1 h (hematoxylin and eosin staining, magnification ×200).

thickness of the mammary alveolus, especially in the 100-μM dose group.

Detection of Inflammatory Cytokine Levels in the Mammary Gland Homogenates

The expression levels of inflammation cytokines (IL-1β, IL-6, and TNF-α) in mammary gland tissue homogenates were measured by an ELISA. LPS challenge caused a significant increase in all three pro-inflammatory mediators compared with the control group (all *p* values <0.001). The

indirubin treatment inhibited the expression of IL-1β, IL-6, and TNF-α in the LPS-stimulated mastitis mouse models in a dose-dependent manner. Furthermore, all levels were significantly lower than those in the LPS groups (*p* values <0.001) (Fig. 3a–c).

Effect of Indirubin on Cell Viability

The MTT assay was used to show that indirubin was not toxic to MMECs. Cell viability was not affected upon exposure to 0–100 nM indirubin, 0.1 % (*v/v*) DMSO (the
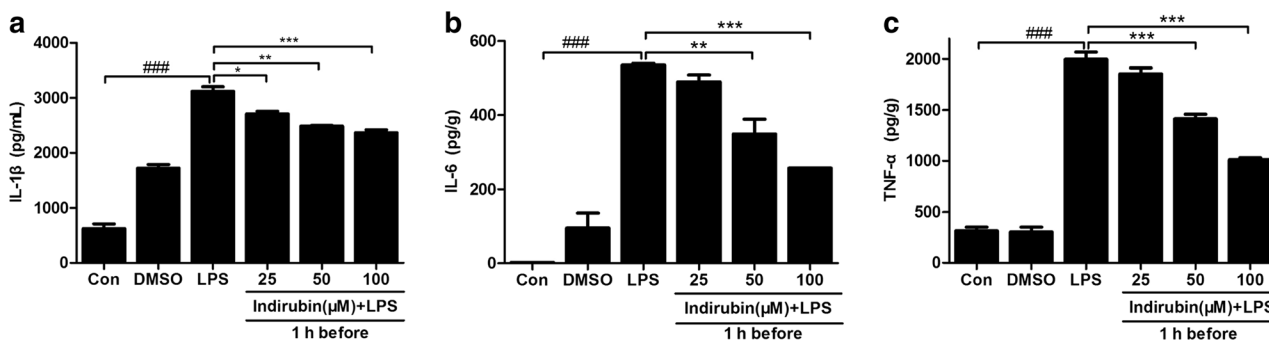
Fig. 3. Effect of indirubin on IL-1β (**a**), IL-6 (**b**), and TNF-α (**c**) in the mammary gland with LPS-stimulated mastitis. Mice were given intraperitoneal injection of indirubin (25, 50, and 100 μM) 1 h before and 12 h after LPS administration. Tissue homogenates were used to evaluate measures with ELISA. The values are presented as the means ± SEM of three independent experiments. ###*p* < 0.001, *versus* control group; *p < 0.05, **p < 0.01, and ***p < 0.001, *versus* LPS group.

maximal level present in the indirubin solution), or 1 μg/mL LPS, for 24 h (Fig. 4). Moreover, the order of addition of LPS and indirubin had no obvious effect on viability.

### Indirubin Reduced the Levels of Pro-inflammatory Cytokines Induced by LPS

We used ELISA and qRT-PCR to measure the levels of the pro-inflammatory cytokines IL-1β, IL-6, and TNF-α. Compared with the control group, LPS significantly increased the levels of these cytokines (all *p* values <0.001). However, these increases were significantly abrogated by indirubin, in a dose-dependent manner (Figs. 5a–c and 6a–c).

Indirubin Inhibited LPS-Induced COX-2 Expression

The COX-2 levels in cell lysates were analyzed by qRT-PCR and western blotting. COX-2 expression was increased by LPS addition, compared with that of the control; indirubin reduced the LPS-induced COX-2 expression with the increased indirubin concentration (Fig. 7a–c).

Effect of Indirubin on TLR4 Expression

TLR4 is a key immune receptor that plays an important role in the regulation of LPS-induced inflammation. We used western blotting to assess the effect of indirubin on TLR4 expression. LPS significantly increased the TLR4 level compared with the control and indirubin-treated groups. TLR4 expression by LPS-exposed MMECs was inhibited by indirubin in a dose-dependent manner (Fig. 8a, b).
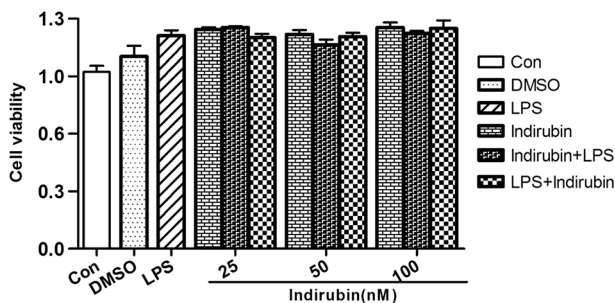
Fig. 4. Effects of indirubin on the cell viability in MMECs. Primary MMECs were cultured with different concentrations of indirubin (25, 50, and 100 nM) in the absence or presence of 1 μg/mL LPS for 24 h. The cell viability was determined by MTT assay. The values are presented as the means ± SEM of three independent experiments.

Indirubin Suppressed the LPS-Induced NF-kB Signaling Pathway

To explore whether the NF-kB pathway mediated indirubin-mediated inhibition of the inflammatory response, the NF-kB and IkBα protein levels were determined by western blotting. The extents of P65 and IkBα phosphorylation were significantly increased after LPS treatment but were reduced by indirubin pretreatment, in a dose-dependent manner (Fig. 9a–c).

Indirubin Suppressed LPS-Induced MAPK Pathways Activated by LPS

The MAPK pathways are controlled by the ERK, JNK, and p38 protein kinases. A western blot was used to determine how indirubin interfered with MAPK pathways; the effects of indirubin on phosphorylation of P38, ERK, and JNK were analyzed. Phosphorylation increased in LPS-stimulated MMECs. Indirubin pretreatment markedly inhibited the LPS-induced increases in P38, ERK, and JNK phosphorylation, in a dose-dependent manner (Fig. 10a–d).

DISCUSSION

Mastitis is characterized by mammary gland inflammation attributable to intramammary bacterial, mycoplasmal, algal, or fungal infection [30]. Antibiotics are frequently used to cure mastitis, but resistance to single or several antibiotics is now commonplace [31]. The abundant mammary epithelial cells are key components of the udder, producing many key milk components supporting the immune system and affording adequate nutrition [32]. LPS induces a large-scale production of pro-inflammatory cytokines, such as TNF-α, and may thus cause tissue damage [33]. In recent years, many traditional Chinese medicine (TCM) extracts have been shown to exert anti-inflammatory effects on mastitis models [34, 35]. Indirubin is one such material, suppressing TNF-induced NF-kB activation [36]. However, indirubin has not yet been tested in animals; this is the first report of the anti-inflammatory effects of indirubin in terms of LPS-induced inflammation [37]; we elucidated the anti-inflammatory mechanisms of indirubin.

Our animal experiment effectively reflects *in vivo* conditions and provides insights into the anti-inflammatory effects of indirubin on LPS-induced mastitis mouse models. Following the LPS challenge, we observed an increase in thickness of the mammary alveolus walls
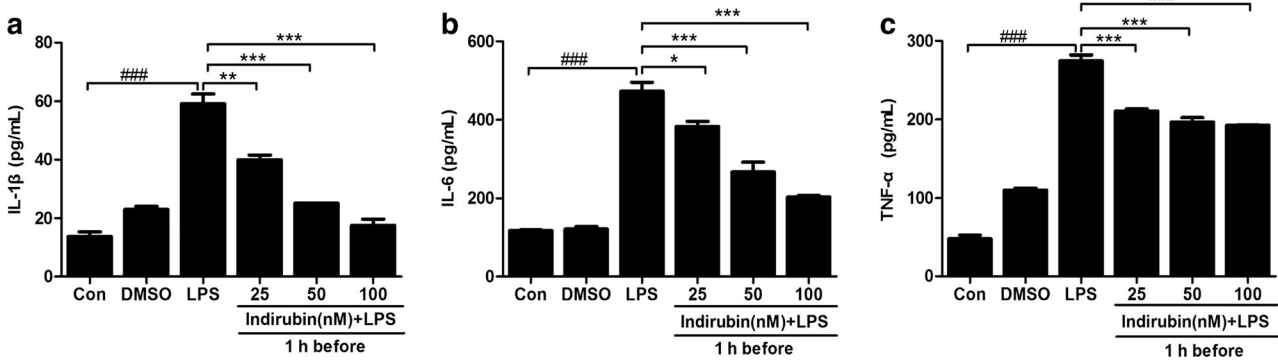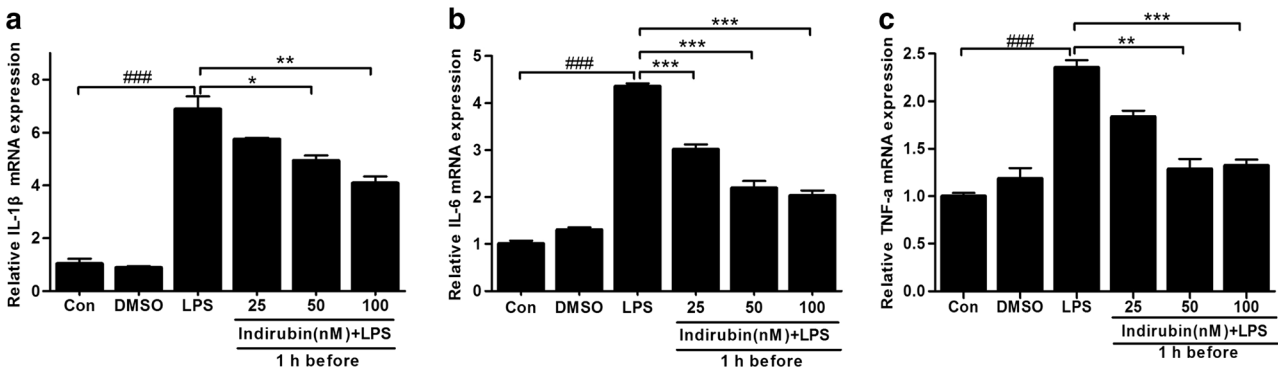
Fig. 5. Effects of indirubin on secretion of IL-1β (**a**), IL-6 (**b**), and TNF-α (**c**) by LPS-stimulated MMECs. Primary MMECs were pretreated with indirubin (25, 50, and 100 nM) for 1 h prior to LPS (1 μg/mL) addition; culture was continued for 24 h. The relative expression levels for IL-1β, IL-6, and TNF-α were measured by ELISA. Data are presented as the means ± SEM ($n = 3$). ### $p < 0.001$, *versus* control group; * $p < 0.05$, ** $p < 0.01$, and *** $p < 0.001$, *versus* LPS group.

compared with the control group, and large numbers of inflammatory cells, such as neutrophils and macrophages, were present in the thickened mammary alveolus. When treated with indirubin, inflammatory symptoms were attenuated (Fig. 2d–f). Compared with the control group, LPS significantly increased the levels of the pro-inflammatory cytokines and was significantly reduced by indirubin in a dose-dependent manner (Fig. 3a–c). Therefore, indirubin has anti-inflammatory effects on LPS-induced mastitis mouse models.

Next, we confirmed that indirubin exerted anti-inflammatory effects on LPS-induced MMECs. Pro-inflammatory cytokines, such as IL-1β, IL-6, IL-10, and TNF-α, are key mediators of most acute and chronic responses to inflammatory diseases. TNF-α and IL-6, the

principal proinflammatory cytokines, are involved in the pathophysiology of endotoxin-induced mastitis, increasing the expression levels of adhesion molecules and triggering the production of reactive oxygen species (ROS) [38–41]. Consequently, we first used ELISA and qRT-PCR to explore whether indirubin suppressed the production of IL-1β, IL-6, and TNF-α in LPS-stimulated MMECs. We next used the MTT assay to confirm that indirubin was not toxic to MMECs up to a concentration of 100 nM (Fig. 4). The DMSO level in this test was <0.1 % (*v/v*), and LPS at 1 μg/mL was also minimally cytotoxic to MMECs. The following experiments reflected these findings. Indirubin (25, 50, and 100 nM) dose-dependently inhibited IL-1β, IL-6, and TNF-α production without a difference with the sequence of indirubin and LPS in LPS-stimulated MMEC. Thus, the


Fig. 6. Effects of indirubin on secretion of IL-1β (**a**), IL-6 (**b**), and TNF-α (**c**) by LPS-stimulated MMECs. Primary MMECs were pretreated with indirubin (25, 50, and 100 nM) for 1 h prior to LPS (1 μg/mL) addition; culture was continued for 24 h. The relative expression levels for IL-1β, IL-6, and TNF-α were measured by qRT-PCR. Data are presented as the means ± SEM ($n = 3$). ### $p < 0.001$, *versus* control group; * $p < 0.05$, ** $p < 0.01$, and *** $p < 0.001$, *versus* LPS group.

a

b

c
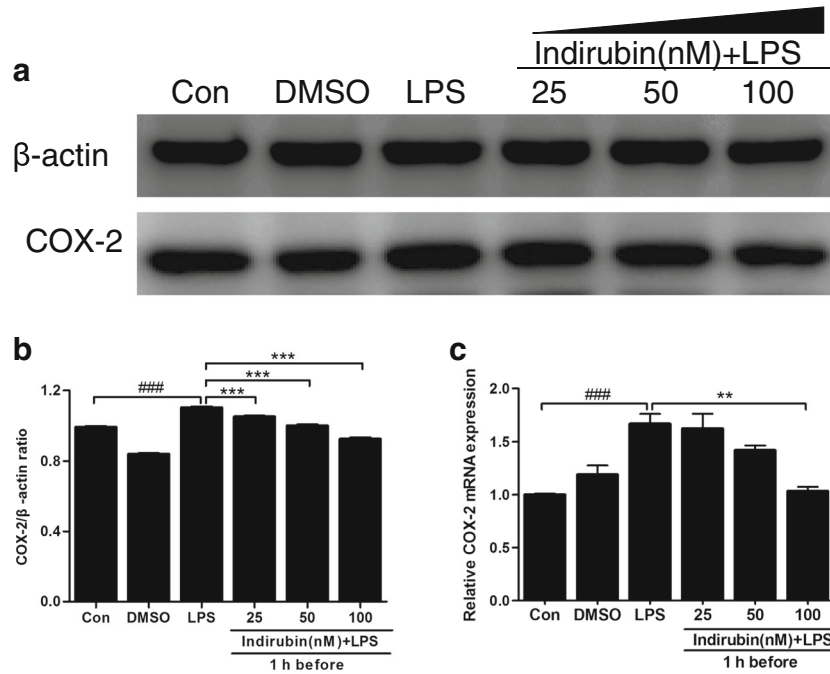
Fig. 7. Anti-inflammatory effects of indirubin on COX-2 expression in LPS-induced MMECs. **a** MMECs were cultured with different concentrations of indirubin (25, 50, and 100 nM) for 1 h and then stimulated with LPS (1 μg/mL) for 24 h. COX-2 was analyzed by western blotting and qRT-PCR. **b** Densitometric analysis of the effects of indirubin on COX-2 expression. Proteins were analyzed by western blotting; β-actin served as an internal control. The values are presented as the means ± SEM ($n = 3$). **c** The relative expression levels for COX-2 were measured by qRT-PCR. Data are presented as the means ± SEM ($n = 3$). $^{###}p < 0.001$, *versus* control group; $^{**}p < 0.01$ and $^{***}p < 0.001$, *versus* LPS group.

inhibitory effects of indirubin on IL-1β, IL-6, and TNF-α expression should reduce the inflammatory responses of MMECs (Figs. 5a–c and 6a–c).

The COX-2 expression level and that of prostaglandin E_2 (PGE_2) serve as pro-inflammatory markers; these materials are interventional targets when treating mastitis [42]. One of the two well-studied isozymes of COX-2 synthesizes the pro-inflammatory PGE_2 when exposed to LPS [43]. We thus assumed that COX-2 inhibition might explain the anti-inflammatory effect of indirubin. COX-2 expression increased significantly after LPS challenge; indirubin pretreatment inhibited this rise in a dose-dependent manner (Fig. 7a–c). Indirubin thus protected MMECs. Thus, indirubin significantly downregulated the synthesis of the pro-inflammatory mediators IL-1β, IL-6, TNF-α, and COX-2, attributable to inactivation of the NF-kB and MAPK signal transduction pathways triggering production of these materials [44–46]. We next use indirubin to pro-protect MMECs and examined the effects of

a

b
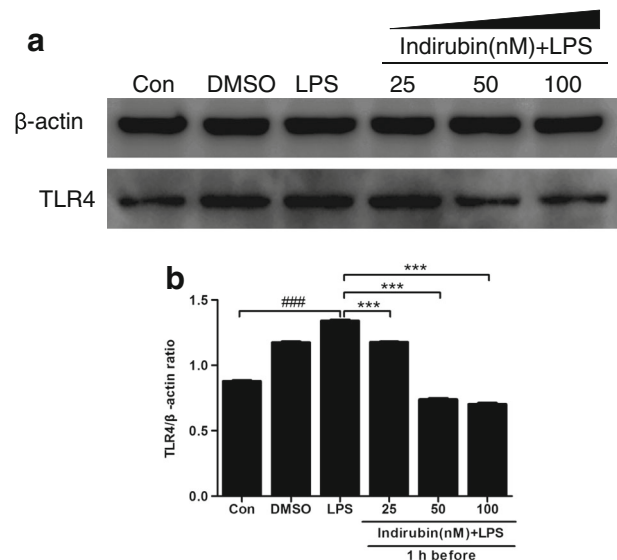
Fig. 8. Effects of indirubin on TLR4 expression in LPS-induced MMECs. **a** Cells were cultured with different concentrations of indirubin (25, 50, and 100 nM) for 1 h and then stimulated with LPS (1 μg/mL) for 24 h. Proteins were analyzed by western blotting. **b** Densitometric analysis of the effects of indirubin on TLR4 expression. Proteins were analyzed by western blotting; β-actin served as an internal control. $^{###}p < 0.001$, *versus* control group; $^{***}p < 0.001$, *versus* LPS group.
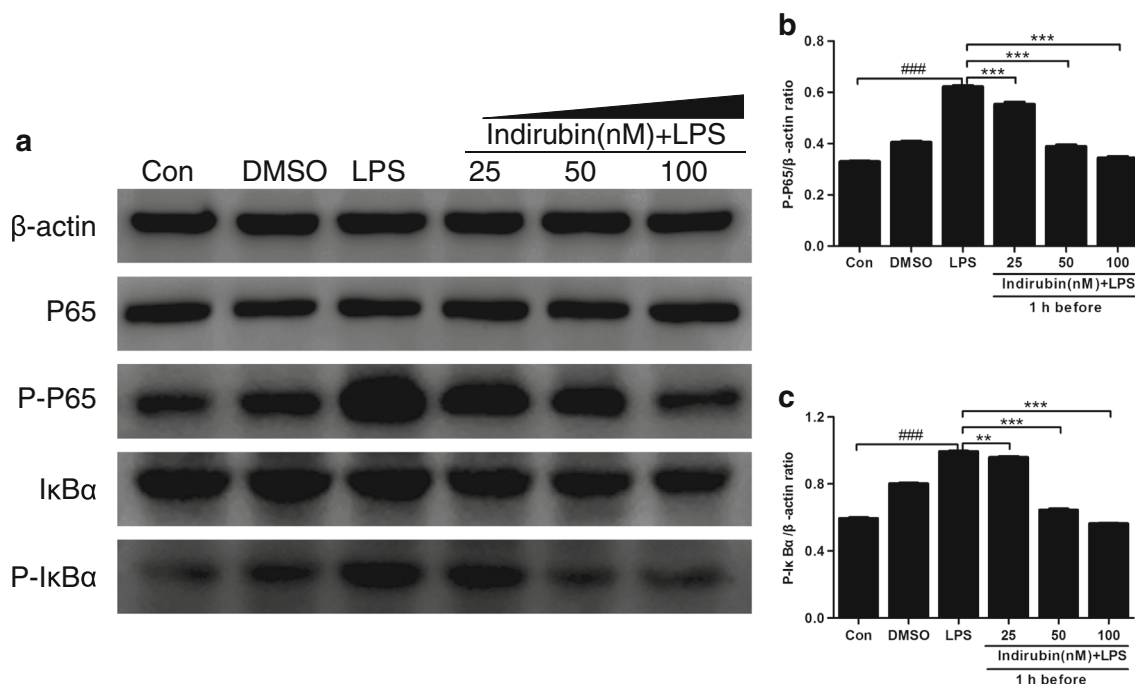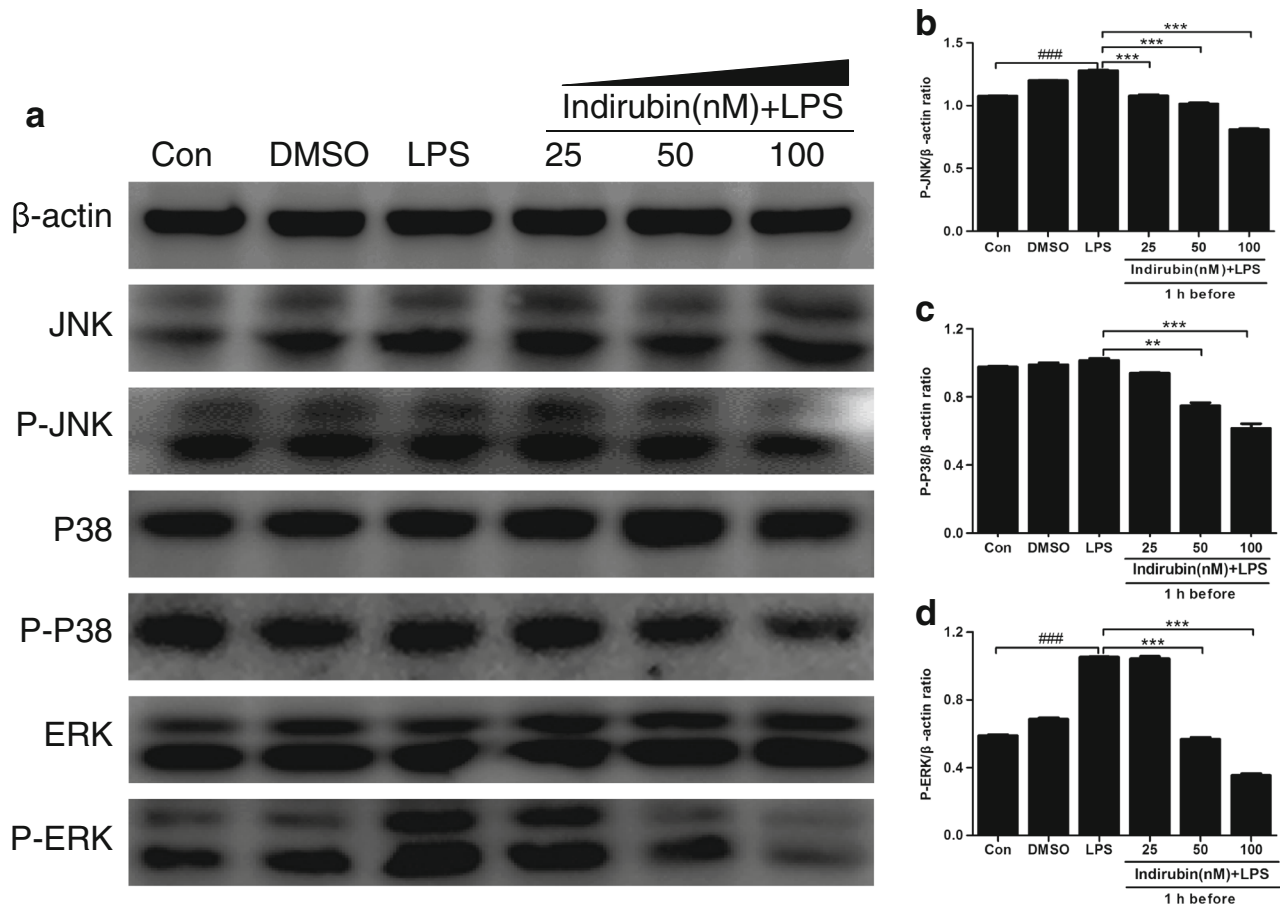
Fig. 9. Effects of indirubin on phosphorylation of IkBα and NF-kB p65 in LPS-induced MMECs. **a** MMECs were pretreated with different concentrations of indirubin (25, 50, and 100 nM) for 1 h and then stimulated with LPS (1 μg/mL) for 24 h; cell lysates were then harvested. Proteins were analyzed by western blotting. **b** Densitometric analysis of the effects of indirubin on phosphorylation of NF-kB p65. **c** Densitometric analysis of the effects of different concentrations of indirubin on phosphorylation of IkBα. The values are presented as the means ± SEM ($n = 3$). [###]$p < 0.001$, *versus* control group; [**]$p < 0.01$ and [***]$p < 0.001$, *versus* LPS group.

indirubin on the TLR4, NF-kB, and MAPK signaling pathways.

Toll-like receptors play important roles in innate immunity; the receptors recognize many pathogens and their pathogenic components (PAMPs) and initiate the innate immune response [47, 48]. Activated TLRs are essential for effective defense against invading pathogens. LPS first activates TLR4 to trigger the downstream NF-kB signaling pathway that regulates cytokine production and the expression of many inflammatory genes [49]. We showed by western blotting that indirubin inhibited TLR4 expression in a dose-dependent manner (Fig. 8a, b). Thus, indirubin weakens inflammation-mediated signaling to a downstream signaling pathway.

The major regulatory transcription factor NF-kB exists as homo- or hetero-dimers with P50 and P65 proteins bound to the inhibitor IkBα; dissociation of the complexes is stimulated by cytokines, free radicals, stress, ultraviolet light, oxidized low-density lipoprotein, and bacterial and viral antigens [50].

Once stimulated, IkBα kinase engages in phosphorylation of NF-kB P65 and ubiquitin-mediated degradation of this product *via* the proteasome pathway. Activated NF-kB enters the nucleus and induces the expression of numerous genes involved in innate and adaptive immune regulation, cell adhesion, inflammatory responses, and anti-apoptotic mechanisms [51, 52]. It is thus not surprising that NF-kB inhibition mitigates the inflammatory response. It is well known that various natural herbs affect anti-inflammatory responses by inhibiting NF-kB signaling [53, 54]. We thus explored whether indirubin inhibited NF-kB P65 phosphorylation and IkBα degradation. The LPS-induced P65 phosphorylation was inhibited by indirubin in a dose-dependent manner *via* inhibition of IkBα degradation (Fig. 9a–c). Thus, indirubin may inhibit IL-1β, IL-6, and TNF-α production by abrogating NF-kB action *via* blockade of IkBα degradation and P65 phosphorylation. Indirubin may thus be useful to inhibit inflammatory reactions.

Fig. 10. Effects of indirubin on MAPK expression in LPS-induced MMECs. **a** Indirubin treatment group after pretreatment with different concentrations of indirubin (25, 50, and 100 nM) for 1 h, and the cells were stimulated with LPS (1 μg/mL) for 24 h and harvested lysates. Proteins were analyzed by western blotting. **b** Densitometric analysis results of the effect of indirubin on phosphorylation of JNK expression. **c** Densitometric analysis results of the effect of indirubin on phosphorylation of P38 expression. **d** Densitometric analysis results of the effect of indirubin on phosphorylation of ERK expression. The cellular proteins were analyzed by western blotting, and β-actin served as an internal control. The values are presented as the means ± SEM ($n = 3$). ###$p < 0.001$, *versus* control group; **$p < 0.01$ and ***$p < 0.001$, *versus* LPS group.

The Myd88-dependent pathways are involved in LPS-induced inflammation. We examined the effects of indirubin on phosphorylation of P38, ERK, and JNK of the MAPK signaling pathway; this pathway controls cytokine synthesis and release during the inflammatory response. Upon activation of MAP kinases, transcription factors in the cytoplasm or nucleus are, in turn, activated, triggering the expression of target genes causing biological responses, including the expression of proinflammatory mediators [55]. We investigated the effects of indirubin on phosphorylation of the ERK, JNK, and P38 MAPKs in LPS-stimulated MMECs; LPS induced ERK, JNK, and p38 MAPK activation. Importantly, indirubin pretreatment significantly suppressed the phosphorylation of P38, ERK, and JNK and may thus inhibit the production of IL-1β, IL-6, and TNF-α, exerting an anti-inflammatory action (Fig. 10a–d).

CONCLUSION

In conclusion, we demonstrated that indirubin exerted anti-inflammatory effects on mice. Indirubin pretreatment attenuated mammary gland histopathological changes and reduced the expression levels of pro-inflammatory genes, including those encoding IL-1β, IL-6, TNF-α, and COX-

2, by inhibiting TLR4 expression and suppressing phosphorylation of IkBα, NF-kB P65, JNK, ERK, and P38. Thus, indirubin may be useful to prevent LPS-induced mastitis.

ACKNOWLEDGMENTS

COMPLIANCE WITH ETHICAL STANDARDS

Conflict of Interest. The authors declare that they have no conflict of interest.

REFERENCES

1. Hu, C., R. Gong, A. Guo, and H. Chen. 2010. Protective effect of ligand-binding domain of fibronectin-binding protein on mastitis induced by *Staphylococcus aureus* in mice. *Vaccine* 28: 4038–4044.

2. De Vliegher, S., L.K. Fox, S. Piepers, S. McDougall, and H.W. Barkema. 2012. Invited review: mastitis in dairy heifers: nature of the disease, potential impact, prevention and control. *Journal of Dairy Science* 95: 1025–1040.

3. Calvinho, L.F., and L. Tirante. 2005. Prevalencia de microorganismos patógenos de mastitis bovinay evolución del estado de salud de la glándula mamaria en Argentina en losúltimos 25 años. *Revista FAVE* 4: 29–40.

4. Watts, J.L. 1988. Etiological agents of bovine mastitis. *Veterinary Microbiology* 16: 41–66.

5. Wellenberg, G.J., W.H. Vander Poel, and J.T. Van Oirschot. 2002. Viral infections and bovine mastitis: a review. *Veterinary Microbiology* 88: 27–45.

6. Guo, M., Y. Cao, T. Wang, X. Song, Z. Liu, E. Zhou, X. Deng, N. Zhang, and Z. Yang. 2014. Baicalin inhibits *Staphylococcus aureus*-induced apoptosis by regulating TLR2 and TLR2-related apoptotic factors in the mouse mammary glands. *European Journal of Pharmacology* 723: 481–488.

7. Burvenich, C., V. Van Merris, J. Mehrzad, A. Diez-Fraile, and L. Duchteau. 2003. Severity of *E. coli* mastitis is mainly determined by cow factors. *Veterinary Research* 34: 521–564.

8. Vangroenweghe, F., P. Rainard, M. Paape, L. Duchateau, and C. Burvenich. 2004. Increase of *Escherichia coli* inoculum doses induces faster innate immune response in primiparous cows. *Journal of Dairy Science* 87: 4132–4144.

9. Yang, Z., E. Zhou, D. Wei, D. Li, Z. Wei, W. Zhang, and X. Zhang. 2014. Emodin inhibits LPS-induced inflammatory response by activating PPAR-γ in mouse mammary epithelial cells. *International Immunopharmacology* 21: 354–360.

10. Reuven, E.M., A. Fink, and Y. Shai. 2014. Regulation of innate immune responses by transmembrane interactions: lessons from the TLR family. *Biochimica et Biophysica Acta* 1838: 1586–1593.

11. Ariyadi, B., N. Isobe, and Y. Yoshimura. 2014. Toll-like receptor signaling for the induction of mucin expression by lipopolysaccharide in the hen vagina. *Poultry Science* 93: 673–679.

12. Kyriakis, John M., and Joseph Avruch. 2001. Mammalian mitogen-activated protein kinase signal transduction pathways activated by stress and inflammation. *Physiological Reviews* 81: 807–869.

13. Lee, J.C., S. Kassis, S. Kumar, A. Badger, and J.L. Adams. 1999. p38 mitogen-activated protein kinase inhibitors—mechanisms and therapeutic potentials. *Pharmacology and Therapeutics* 82: 389–397.

14. Wang, W., D.J. Liang, X.J. Song, T. Wang, Y. Cao, Z. Yang, and N. Zhang. 2015. Magnolol inhibits the inflammatory response in mouse mammary epithelial cells and a mouse mastitis model. *Inflammation* 38: 16–26.

15. Kunikata, T., T. Tatefuji, H. Aga, K. Iwaki, M. Ikeda, and M. Kurimoto. 2000. Indirubin inhibits inflammatory reactions in delayed-type hypersensitivity. *European Journal of Pharmacology* 410: 93–100.

16. Ma, M.Z., and B.Y. Yao. 1983. Progress in indirubin treatment of chronic myelocytic leukemia. *Journal of Traditional Chinese Medicine* 3: 245–248.

17. Blažević, T., E.H. Heiss, A.G. Atanasov, J.M. Breuss, V.M. Dirsch, and P. Uhrin. 2015. Indirubin and indirubin derivatives for counteracting proliferative diseases. *Evidence-Based Complementary and Alternative Medicine* 2015: 1–12.

18. Kim, J.K., E.K. Shin, Y.H. Kang, and J.H.Y. Park. 2011. Indirubin-3-monoxime, a derivative of a Chinese antileukemia medicine, inhibits angiogenesis. *Journal of Cellular Biochemistry* 112: 384–1391.

19. Ravichandran, K., A. Pal, and R. Ravichandran. 2010. Effect of indirubin-3-monoxime against lung cancer as evaluated by histological and transmission electron microscopic studies. *Microscopy Research and Technique* 73: 1053–1058.

20. Perabo, F.G., G. Landwehrs, C. Frossler, D.H. Schmidt, and S.C. Mueller. 2011. Anti-proliferative and apoptosis inducing effects of indirubin-3-monoxime in renal cell cancer cells. *Urologic Oncology* 29: 815–820.

21. Varela, A.T., A.M. Simoes, J.S. Teodoro, F.V. Duarte, A.P. Gomes, C.M. Palmeira, and A.P. Rolo. 2010. Indirubin-3-oxime prevents hepatic I/R damage by inhibiting GSK-3beta and mitochondrial permeability transition. *Mitochondrion* 10: 456–463.

22. Polychronopoulos, P., P. Magiatis, A.L. Skaltsounis, V. Myrianthopoulos, E. Mikros, A. Tarricone, A. Musacchio, S.M. Roe, L. Pearl, M. Leost, P. Greengard, and L. Meijer. 2004. Structural basis for the synthesis of indirubins as potent and selective inhibitors of glycogen synthase kinase-3 and cyclin-dependent kinases. *Journal of Medicinal Chemistry* 47: 935–946.

23. Li, D., N. Zhang, Y. Cao, W. Zhang, G. Su, Y. Sun, and M. Guo. 2013. Emodin ameliorates lipopolysaccharide-induced mastitis in mice by inhibiting activation of NF-kB and MAPKs signal pathways. *European Journal of Pharmacology* 705: 79–85.

24. Ip, M.M., P.A. Masso-Welch, S.F. Shoemaker, W.K. Shea-Eaton, and C. Ip. 1999. Conjugated linoleic acid inhibits proliferation and induces apoptosis of normal rat mammary epithelial cells in primary culture. *Experimental Cell Research* 250: 22–34.

25. Livak, K.J., and T.D. Schmittgen. 2001. Analysis of relative gene expression data using real-time quantitative PCR and the $2-\Delta\Delta CT$ method. *Methods* 25: 402–408.

26. Chen, S.T., J.Y. Li, Y. Zhang, X. Gao, and H. Cai. 2012. Recombinant MPT83 derived from Mycobacterium tuberculosis induces cytokine production and upregulates the function of mouse macrophages through TLR2. *The Journal of Immunology* 188: 668–677.

27. Zhang, Q., Y. Yang, S. Yan, J. Liu, Z. Xu, J. Yu, and M. Jin. 2015. A novel pro-inflammatory protein of *Streptococcus suis* 2 induces the Toll-like receptor 2-dependent expression of pro-inflammatory cytokines in RAW 264.7 macrophages via activation of ERK1/2 pathway. *Frontiers in Microbiology* 6: 178.

28. Wang, T., M. Guo, X. Song, Z. Zhang, H. Jiang, W. Wang, and N. Zhang. 2014. Stevioside plays an anti-inflammatory role by regulating the NF-kB and MAPK pathways in S. aureus-infected mouse mammary glands. *Inflammation* 37: 1837–1846.

29. Nayak, L., L. Goduni, Y. Takami, N. Sharma, P. Kapil, M.K. Jain, and G.H. Mahabeleshwar. 2013. Kruppel-like factor 2 is a transcriptional regulator of chronic and acute inflammation. *The American Journal of Pathology* 182: 1696–1704.

30. Zhao, X., and P. Lacasse. 2008. Mammary tissue damage during bovine mastitis causes and control. *Journal of Animal Science* 86: 57–65.

31. Babra, C., J.G. Tiwari, G. Pier, T.H. Thein, R. Sunagar, S. Sundareshan, S. Isloor, Na R. Hegde, S. de Wet, M. Deighton, J. Gibson, P. Costantino, J. Wetherall, and T. Mukkur. 2013. The persistence of biofilm-associated antibiotic resistance of *Staphylococcus aureus* isolated from clinical bovine mastitis cases in Australia. *Folia Microbiologica* 58: 469–474.

32. Senegas, A., O. Villard, A. Neuville, L. Marcellin, A.W. Pfaff, T. Steinmetz, M. Mousli, J.P. Klein, and E. Candolfi. 2009. Toxoplasma gondii-induced foetal resorption in mice involves interferon-mamma-induced apoptosis and spiral artery dilation at the matermofoetal interface. *International Journal for Parasitology* 39: 481–487.

33. Takahashi, K., H.S.W. Schaffer, and J. Azuma. 1992. Effect of taurine on intracellular calcium dynamics of cultured myocardial cells during the calcium paradox. *Advances in Experimental Medicine and Biology* 315: 153–161.

34. Li, F., D. Liang, Z. Yang, T. Wang, W. Wang, X. Song, M. Guo, E. Zhou, D. Li, Y. Cao, and N. Zhang. 2013. Astragalin suppresses inflammatory responses via down-regulation of NF-kB signaling pathway in lipopolysaccharide-induced mastitis in a murine model. *International Immunopharmacology* 17: 478–482.

35. Song, X., W. Zhang, T. Wang, H. Jiang, Z. Zhang, Y. Fu, Z. Yang, Y. Cao, and N. Zhang. 2014. Geniposide plays an anti-inflammatory role via regulating TLR4 and downstream signaling pathway in lipopolysaccharide-induced mastitis in mice. *Inflammation* 37: 1588–98.

36. Ding, Y., A. Qiao, and G.H. Fan. 2014. Indirubin-3′-monoxime rescues spatial memory deficits and attenuates beta-amyloid-associated neuropathology in a mouse model of Alzheimer's disease. *Neurobiology of Disease* 39: 156–168.

37. Hoessel, R., S. Leclerc, J.A. Endicott, et al. 1999. Indirubin, the active constituent of a Chinese antileukaemia medicine, inhibits cyclin-dependent kinases. *Nature Cell Biology* 1: 60–67.

38. Higashimoto, T.A., C.L. Panopoulos, and E. Zandi. 2006. TNF alpha induces chromosomal abnormalities independent of ROS through IKK, JNK, p38 and caspase pathways. *Cytokine* 34: 39–50.

39. Yoon, W.J., J.Y. Moon, J.Y. Kang, N.H. Lee, and C.G. Hyun. 2010. Neolitsea sericea essential oil attenuates LPS-induced inflammation in RAW 264.7 macrophages by suppressing NF-kappa B and MAPK activation. *Natural Product Communications* 5: 1311–1316.

40. Ho, A.W., C.K. Wong, and C.W. Lam. 2008. Tumor necrosis factor alpha up-regulates the expression of CCL2 and adhesion molecules of human proximal tubular epithelial cells through MAPK signaling pathways. *Immunobiology* 213: 533–544.

41. Shalaby, M.R., B.B. Aggarwal, E. Rinderknecht, L.P. Svedersky, B.S. Finkle, and M.A. Palladino Jr. 1985. Activation of human polymorphonuclear neutrophil functions by interferon-gamma and tumor necrosis factors. *Journal of Immunology* 135: 2069–2073.

42. Morita, I. 2002. Distinct functions of COX-1 and COX-2. *Prostaglandins & Other Lipid Mediators* 68–69: 165–175.

43. Strandberg, Y., C. Gray, T. Vuocolo, L. Donaldson, M. Broadway, and R. Tellam. 2005. Lipopolysaccharide and lipoteichoic acid induce different innate immune responses in bovine mammary epithelial cells. *Cytokine* 1: 72–86.

44. Duntas, L.H. 2009. Selenium and inflammation: underlying anti-inflammatory mechanisms. *Hormone and Metabolic Research* 41: 443–447.

45. Vunta, H., B.J. Belda, R.J. Arner, C. Channa Reddy, John P. Vanden Heuvel, and K. Sandeep Prabhu. 2008. Selenium attenuates pro-inflammatory gene expression in macrophages. *Molecular Nutrition & Food Research* 52: 1316–1323.

46. Pfaffl, M.W., S.L. Wittmann, H.H. Meyer, and R.M. Bruckmaier. 2003. Gene expression of immunologically important factors in blood cells, milk cells, and mammary tissue of cows. *Journal of Dairy Science* 86: 538–545.

47. Akira, S., K. Takeda, and T. Kaisho. 2001. Toll-like receptors: critical proteins linking innate and acquired immunity. *Nature Immunology* 2: 675–680.

48. Beutler, B., K. Hoebe, X. Du, and R.J. Ulevitch. 2003. How we detect microbes and respond to them: the Toll-like receptors and their transducers. *Journal of Leukocyte Biology* 74: 479–485.

49. Vunta, H., F. Davis, U.D. Palempalli, D. Bhat, R.J. Arner, J.T. Thompson, and K.S. Prabhu. 2007. The anti-inflammatory effects of selenium are mediated through 15-deoxy-Δ12, 14-prostaglandin J2 in macrophages. *Journal of Biological Chemistry* 282: 17964–17973.

50. Oh, Y.C., W.K. Cho, Y.H. Jeong, G.Y. Im, A. Kim, Y.H. Hwang, and J.Y. Ma. 2012. A novel herbal medicine KIOM-MA exerts an anti-inflammatory effect in LPS-stimulated RAW 264.7 macrophage cells. *Evidence-Based Complementary and Alternative Medicine* 2012: 1–11.

51. Hayden, M.S., and S. Ghosh. 2012. NF-kappa B, the first quarter-century: remarkable progress and outstanding questions. *Genes and Development* 6: 203–234.

52. Vallabhapurapu, S., and M. Karin. 2009. Regulation and function of NF-kappa B transcription factors in the immune system. *Annual Review of Immunology* 27: 693–733.

53. Liang, C.J., C.W. Lee, H.C. Sung, Y.H. Chen, Y.C. Chiang, H.Y. Hsu, and Y.L. Chen. 2014. Ganoderma lucidum polysaccharides reduce lipopolysaccharide-induced interleukin-1β expression in cultured smooth muscle cells and in thoracic aortas in mice. *Evidence-Based Complementary and Alternative Medicine* 2014: 305149.

54. Remppis, A., F. Bea, H.J. Greten, A. Buttler, H. Wang, Q. Zhou, and E. Blessing. 2010. Rhizoma coptidis inhibits LPS-induced MCP-1/CCL2 production in murine macrophages via an AP-1 and NF-kB-dependent pathway. *Mediators of Inflammation* 2010: 194896.

55. Kaminska, B. 2005. MAPK signalling pathways as molecular targets for anti-inflammatory therapy—from molecular mechanisms to therapeutic benefits. *Biochimica et Biophysica Acta* 1754: 253–262.